

FIRST MODEL OF THE EDGE-FOCUSING WIGGLER FOR SASE

S. Kashiwagi[#], K. Kobayashi, T. Noda, R. Kato, G. Isoyama,
ISIR, Osaka University, 8-1 Mihogaoka, Ibaraki, Osaka, Japan
S. Yamamoto and K. Tsuchiya

Institute of Materials Structure Science, KEK, 1-1 Oho, Tsukuba, Ibaraki, Japan

Abstract

The first model of the edge-focusing (EF) wiggler, which produces the strong transverse focusing field incorporated with the normal wiggler field, has been fabricated to evaluate its performance. It is a five-period planar wiggler with an edge angle of 2 degrees and a period length of 60 mm. The magnetic field in the wiggler is measured using Hole probes at four different wiggler gaps. It is experimentally confirmed that a high field gradient of 1.0 T/m is realized along the beam axis in the EF wiggler.

INTRODUCTION

A conventional planar wiggler of the horizontal oscillation type focuses the electron beam in the vertical direction, but does not focus in the horizontal direction. If the beam is injected to the wiggler with the matching condition in the vertical direction, the vertical beam size will remain constant as it moves along the wiggler. In the horizontal direction, however, no focusing force exists and the beam size will increase and diverge if the external focusing force is not provided. Various schemes have been proposed or investigated to provide the focusing force in the both directions in the wiggler for Self-Amplified Spontaneous Emission (SASE) in the short wavelength region so that the beam size is kept small over the whole length of the very long wiggler [3-9]. In these schemes, either pole faces are shaped or permanent magnet blocks are added in the wiggler gap, in order to produce the field gradient for focusing the beam. The magnet gap of the wiggler is sacrificed in some of these methods or the good field region is limited in the other methods.

As a new method for the integrated-focusing, we proposed the Edge-Focus (EF) wiggler, which can produce the high magnetic field gradient superimposed on the normal wiggler field [1,2]. The EF wiggler has an advantage that the strong field gradient can be produced with no obstacles in the wiggler gap and the good field region is as large as that of the normal wiggler field. It can be used not only for SASE experiments but also for FEL in order to enhance the gain. As a next step of our proposal, we have fabricated the first experimental model of the EF wiggler. In the fabrication process of this model wiggler, we developed a new method to make a low-error wiggler without adjustment of the magnetic field by trial and error, and reported at the preceding FEL conference [2]. The wiggler parameters of the first model have been

[#]E-mail: shigeruk@sanken.osaka-u.ac.jp

chosen to meet requirements from our SASE experiment in the far-infrared region being conducted at the Institute of Scientific and Industrial Research (ISIR), Osaka University [10,11]. In this paper, we will describe the first model of the EF wiggler and report results of the magnetic field measurement for the EF wiggler.

FIRST MODEL OF THE EDGE-FOCUSING WIGGLER

The EF wiggler is basically a Halbach type wiggler made only of permanent magnet blocks, but their shapes are not rectangular parallelepipeds. The magnet blocks of the EF wiggler with vertical magnetization have a trapezoidal shape with an edge angle ϕ , while those with longitudinal magnetization have a parallelogram shape with the same angle (shown in Figure 1). The average focusing force of the EF wiggler can be calculated using the simple model with the edge angle for the bending magnets. In the simple model based on transfer matrices, the focusing force in the EF wiggler (horizontal oscillation type) is approximately given by

$$k_x = \frac{1}{B\rho} \left(\frac{dB_y}{dx} \right) = \frac{4e}{m_0c} \frac{B_0}{\gamma} \times \frac{\phi}{\lambda_w} \quad (1)$$

$$k_y = k_0 - k_x = \frac{8-\pi}{3\pi} \left(\frac{e}{m_0c} \right)^2 \left(\frac{B_0}{\gamma} \right)^2 - k_x \quad (2)$$

where k_0 is the natural focusing force of the wiggler for the vertical direction and $k_0 = k_x + k_y$. From Eq. (1), the field gradient is given by

$$\frac{dB_y}{dx} = 4 \frac{B_0}{\lambda_w} \phi. \quad (3)$$

The field gradient is approximately proportional to the edge angle and hence the focusing force along the wiggler can be easily adjusted with the edge angle ϕ .

The first model of the EF wiggler consists of five-periods with the period length $\lambda_w = 60$ mm and the edge angle $\phi = 2$ degrees. The main parameters of the model wiggler are listed in Table 1. The magnetic gap is mechanically fixed, but it can be easily changed by changing columns supporting the upper magnet array. The permanent magnet is Nd-Fe-B with the residual induction of 1.32 T, and the standard dimensions of the magnet blocks are $2a \times 2b \times 2c = 100 \times 20 \times 15$ mm³. The peak magnetic field of the wiggler at $g = 30$ mm is

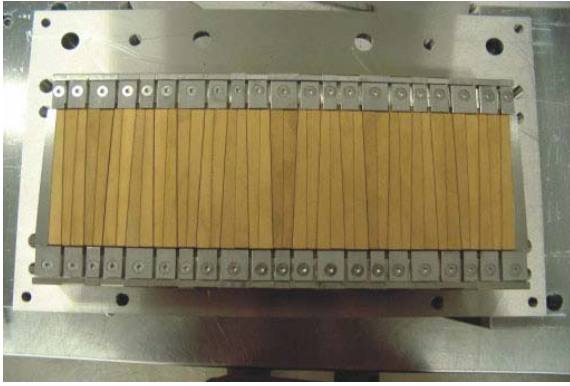


Figure 1: Magnet array of the first model of the EF wiggler. The vertical magnetization magnet blocks have a trapezoidal shape, while those with longitudinal magnetization have a parallelogram shape.

Table 1: Main parameters of the model EF wiggler

Block size ($2a \times 2b \times 2c$)	$100 \times 20 \times 7.5 \text{ mm}^3$
Gap	30 mm
Number of periods	5 periods
Residual induction of magnet	$B_r = 1.32 \text{ T}$
Peak magnetic field (analytical)	$B_0 = 0.43 \text{ T}$
Edge angle	$\phi = 2.0^\circ$
Averaged field gradient ($\phi = 2^\circ$)	$dB_y/dx = 1.0 \text{ T/m}$

calculated using a 3D program to be 0.43 T [12]. The field gradient of the model wiggler averaged over a wiggler period is about 1 T/m at 30 mm gap and the edge angle of 2 degrees. This edge angle is chosen so that the double focusing is realized in both the vertical and the horizontal directions for the 11.5 MeV electron beam.

FIELD MEASUREMENT OF THE WIGGLER

In order to evaluate performance of the EF wiggler, the magnetic field has been measured at the High Energy Accelerator Research Organization (KEK), using a magnetic sensor with two Hole probes for simultaneous measurement of the vertical and the horizontal field components, which is mounted in a small oven to control the temperature of the sensor. Owing to the temperature control, an accuracy of the magnetic field measurement is achieved to be about 0.1 Gauss. The Hole probes were calibrated using NMR. The magnetic sensor is mounted on a 3-axis linear stage, with which it is scanned along the wiggler axis and its transverse position (x-y position) is adjusted. Figure 2 shows the experimental setup for the magnetic field measurement of the EF wiggler. We measure the magnetic field simultaneously in the horizontal and the vertical directions using this measurement system and make the field mapping in the wiggler.

Figure 3 shows the vertical magnetic field $B_y(z)$ measured at the 30 mm gap along the wiggler axis from -300 mm to +300 mm. We calculate the three-dimensional magnetic field in the EF wiggler numerically with the magnetic charge method [12] and compare the calculated values with the measured ones. The calculated values agree quite well with the measured values except for the absolute value. The measured magnetic field at the middle of the wiggler axis (the peak magnetic field) is approximately 4200 Gauss. This value is about 2% smaller than a calculated value. This small difference seems to come from short and shallow steps at the both ends of the magnet blocks for mechanical clamping to folders, which are not taken into account in the calculation.

To obtain the field gradient (dB_y/dx) of the model wiggler, we measure the magnetic field along the

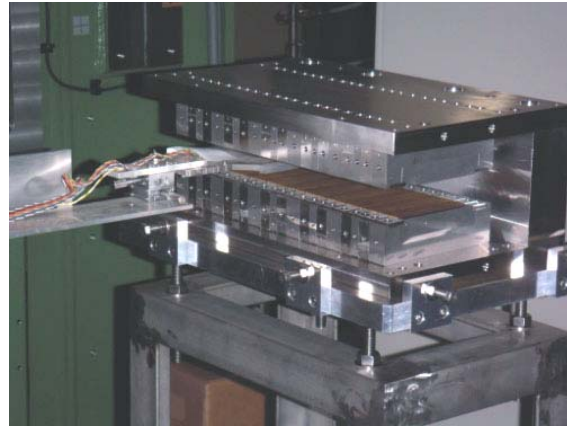


Figure 2: Photograph of the setup for the magnetic field measurement of the EF wiggler at KEK.

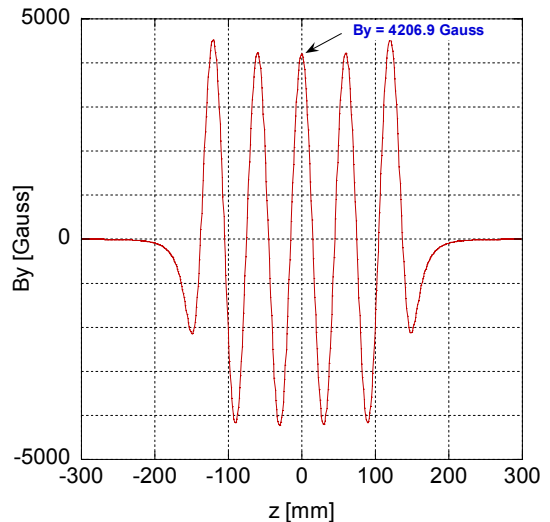


Figure 3: Measured vertical magnetic field $B_y(z)$ along the central wiggler axis.

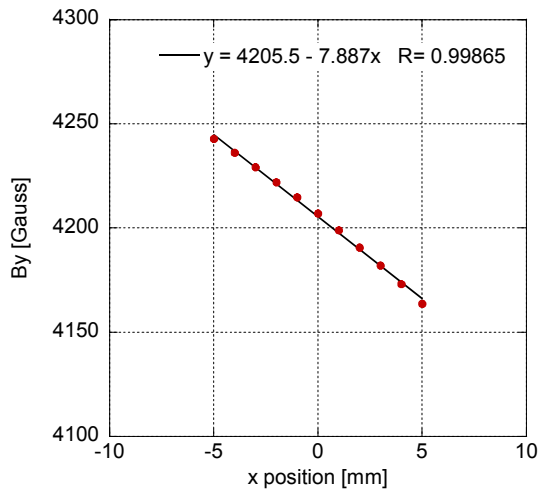


Figure 4: Measured magnetic field $B_y(x, y=0)$ as a function of the horizontal position at the middle of the wiggler.

longitudinal axis at several transverse positions. Figure 4 shows the measured vertical magnetic field along the x-axis (horizontal) at the middle of the model wiggler, where the vertical magnetization block is located. The vertical magnetic field changes linearly with the horizontal position over the width of the wiggler and the slope is steep. The field gradient is derived with linear fitting of the data points as shown in Figure 4. The electron beam receives the focusing force produced by this large field gradient.

We measure the magnetic field at wiggler gaps $g = 30, 40, 50,$ and 60 mm by changing columns supporting the upper magnet array and derive the transverse field gradient as a function of the wiggler gap. The field gradient averaged over the wiggler periods is shown in Figure 5, together with the peak magnetic field. The solid circles and open circles show the measured peak magnetic field and the averaged field gradient of the EF wiggler, respectively. The solid line and the dashed line show the peak magnetic field and the averaged field gradient calculated with the 3D program, respectively. The measured values are in good agreement with the numerical calculation as shown in Figure 5. The peak magnetic field of the wiggler decreases exponentially with increasing the wiggler gap and the averaged field gradient also decreases exponentially as shown in Figure 5, but the slope for the field gradient is gentler than that for the peak magnetic field. The peak field at the gap 60 mm decreases to one fifth of the value at 30 mm, whereas the field gradient at 60 mm decreases to only a half of the value at 30 mm. This behaviour is favourable in the view of the beam dynamics in the wiggler.

The simple model based on transfer matrices fails to explain this behaviour, because the field gradient of the EF wiggler given by Eq. (3) is proportional to the peak magnetic field. We think that this is because the variation

of the fringe field with the wiggler gap is not taken into account in the simple model calculation for the field gradient of the EF wiggler. This indicates that the field measurement and the 3D magnetic field calculation of the wiggler are important to understand the field distribution in the wiggler.

The EF wiggler can produce the high field gradient in the wiggler and the sum of the vertical focusing force and the horizontal one is constant and equal to the natural focusing force, as shown by Eq. (2). The electron beam is simultaneously focused in the both directions with the weak focusing scheme if the horizontal focusing force generated by the edge angle is smaller than the natural focusing of the wiggler, which is realized when the electron beam energy is low and the peak magnetic field of the wiggler is high as well as the edge angle is not very large. If the horizontal focusing force of the EF wiggler is larger than the natural focusing, the defocusing force is provided in the vertical direction. In this case, the strong focusing scheme can be applied to focus the electron beam in the both directions, using two kinds of EF wigglers with positive and negative edge angles. The peak field decreases exponentially with increasing the magnetic gap and accordingly the natural focusing force also decreases exponentially. When the wiggler field becomes weak, the double focusing condition may not be fulfilled at larger gaps. It is, therefore, important to carefully choose the focusing scheme, either the weak focusing or the strong focusing. As an example of the double focusing, the square roots of the betatron functions in the 2m-long conventional planar wiggler with the edge angle $= 0$ deg. and in the EF wiggler with the edge angle of 1 degree are shown in Figure 6. The EF wiggler can produce focusing forces in the both directions and the

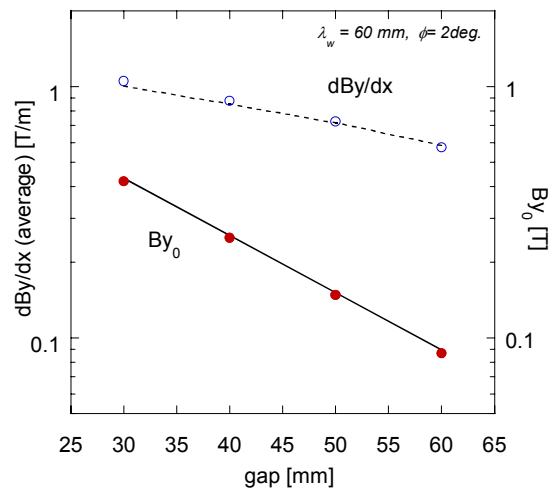


Figure 5: Peak magnetic field and the field gradient of the EF wiggler as a function of the wiggler gap. The solid circles and the open circles show the measured peak magnetic field and the average field gradient over the wiggler period, respectively. The solid and the dashed lines show calculation using the 3D program.

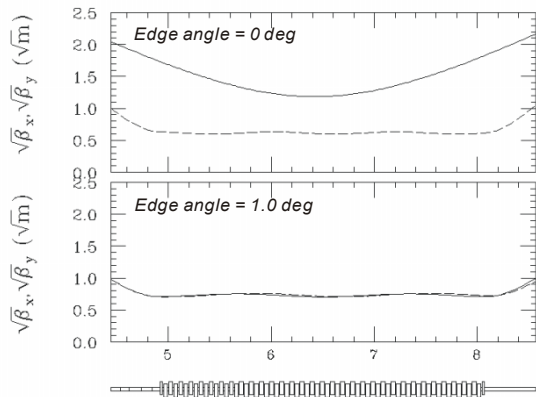


Figure 6: Square root of the betatron function for the conventional planar wiggler with no edge and the EF wiggler with the edge angle of one degree. The solid and the dashed lines show the horizontal and vertical betatron functions, respectively.

betatron functions can be made small and almost constant through the wiggler, using the matching conditions. For the conventional planar wiggler, the horizontal focusing force has to be provided with external quadrupole magnets and hence the beam cannot be focused as small as it is in the double focusing scheme. The EF wiggler can be used to enhance the gain of SASE and FEL.

CONCLUSION

In order to advance the development of the EF wiggler, which we had proposed, we fabricated the first model of the EF wiggler. The magnetic field in the wiggler was measured using Hole probes at four wiggler gaps. It was experimentally confirmed that a high field gradient of about 1.0 T/m was realized along the beam axis in the EF wiggler, which was superimposed on the normal wiggler field. We obtained the relation between the magnetic field gradient and the magnetic gap of the EF wiggler. The field gradient decreases with increasing the magnet gap more slowly than the peak magnetic field does, which is

favourable in view of the beam focusing in the wiggler. We experimentally evaluated the performance of the EF wiggler with the magnetic field measurement. We plan to further study characteristics of the EF wiggler.

ACKNOWLEDGEMENT

The authors would like to thank Mrs. T. Koda and K. Okihira of NEOMAX Co., Ltd. for their help on the fabrication and the magnetic field measurement of the EF wiggler. This research was partly supported by the Joint Development Research at the High Energy Accelerator Research Organization (KEK), 2003-17, 2003 and the Ministry of Education, Science, Sports and Culture, Grant-in-Aid for Exploratory Research, 15654036, 2003&2004.

REFERENCES

- [1] G. Isoyama et al., Nucl. Instr. and Meth. A 507 (2003) 234
- [2] S. Kashiwagi et al., Nucl. Instr. and Meth. A 528 (2004) 203
- [3] J. Pfluger and Yu. M. Nikitina, Nucl. Instr. and Meth. A 381 (1996) 554
- [4] M. Takabe et al., Nucl. Instr. and Meth. A 331 (1993) 736
- [5] Y. Tsunawaki et al., Nucl. Instr. and Meth. A 304 (1991) 753
- [6] M. Shiho et al., Nucl. Instr. and Meth. A 304 (1991) 141
- [7] A. A. Varfolomeev and A. H. Hairetdinov, Nucl. Instr. and Meth. A 341 (1994) 462
- [8] A. A. Varfolomeev, et al., Nucl. Instr. and Meth. A 358 (1995) 70
- [9] Ross D. Schlueter, Nucl. Instr. and Meth. A 358 (1995) 44
- [10] R. Kato, et al., Nucl. Instr. and Meth. A 407 (1998) 157
- [11] R. Kato, et al., Nucl. Instr. and Meth. A 445 (2003) 164
- [12] G. Isoyama, Rev. Sci. Instrum., Vol. 60, No. 7 (1989) 1826